The Generalized heat function

Richard J. Greatbatch[1] and Xiaoming Zhai[1]

Received 23 July 2007; revised 20 September 2007; accepted 3 October 2007; published 1 November 2007.

[1] A generalized heat function is defined for diagnosing the pathways by which heat is carried by the ocean. In contrast to previous work, our generalized heat function varies along an isentrope only in the presence of mixing. The generalized heat function is diagnosed using the Levitus global ocean data set, net northward heat transport based on the data set of Grist and Josey, and different specifications for mixing in the ocean. The separation between the heat flux carried by the shallow wind driven cells and the deep overturning circulation is clearly revealed, with up to 0.4 PW being associated with the spreading of North Atlantic Deep Water. The importance of eddy-induced mixing near the surface of the Southern Ocean is evident. **Citation:** Greatbatch, R. J., and X. Zhai (2007), The Generalized heat function, *Geophys. Res. Lett.*, *34*, L21601, doi:10.1029/2007GL031427.

1. Introduction

[2] *Boccaletti et al.* [2005] recently introduced the "heat function" in an effort to try pin down the pathways by which heat is carried by the ocean. The traditional view has been that heat transport in the North Atlantic is dominated by the meridional overturning circulation (MOC) associated with the southward spreading of North Atlantic Deep Water from its formation sites in the Labrador and Nordic Seas [*Bryan*, 1962; *Hall and Bryden*, 1982; *Roemmich and Wunsch*, 1985], and there has also been much speculation about the role of the MOC in climate change [see, e.g., *Alley et al.*, 2003; *Wunsch*, 2006]. *Boccaletti et al.* [2005], on the other hand, argue that in the North Atlantic, the shallow wind-driven overturning cells account for roughly half the total heat transport. Furthermore, they emphasize the role of the shallow wind driven cells for transporting most of the heat carried by the global ocean. Here, we review and extend the heat function as discussed by *Boccaletti et al.* [2005]. By making use of an integral constraint going back to *Walin* [1982] [see *Greatbatch et al.*, 2007], we show that a "generalized heat function" can be defined in a unique and physically appealing way that differs from the more empirical approach taken by *Boccaletti et al.* [2005] and avoids the redundancy discussed by those authors. We then diagnose the new heat function using the atlas of *Levitus et al.* [1998], net northward heat transport specified using the work by *Grist and Josey* [2003], and different specifications for the ocean mixing.

2. Theoretical Background

2.1. The Heat Function as by *Boccaletti et al.* [2005]

[3] In a statistically steady state, and after zonal and time averaging at fixed height, the equation for the zonally-averaged ocean heat budget can be written [see *Greatbatch et al.*, 2007] as

$$\nabla \cdot \mathbf{H} = 0, \tag{1}$$

where

$$\mathbf{H} = L_w(\mathbf{u}^*\bar{T} - \mathbf{K}\nabla\bar{T}). \tag{2}$$

[4] Here the overbar denotes an averaged quantity, L_w is the zonal width of the ocean as a function of latitude and depth, T is the potential temperature, $\mathbf{u}^*$ is the "residual mean" velocity, i.e. the sum of the Eulerian mean and eddy-induced transport velocity [see *Gent et al.*, 1995], and $\mathbf{K}$ is the diffusion tensor. (Note that the factor of ρc_p has been neglected here, and later, for simplicity). $\mathbf{H}$ is the ocean heat transport vector and the vertical integral of the northward component of $\mathbf{H}$ gives the total northward heat transport at any given latitude. Since $\nabla \cdot \mathbf{H} = 0$, it is possible to define a stream function, ϕ_{raw} such that $\mathbf{H} = -\mathbf{i} \times \nabla\phi_{raw}$ where $\mathbf{i}$ is a unit vector in the eastward direction. However, as noted by *Boccaletti et al.* [2005], there is redundancy in $\mathbf{H}$. To understand this, we note that since $\nabla \cdot (L_w\mathbf{u}^*) = 0$, we can define a stream function, ψ, for $L_w\mathbf{u}^*$ - the stream function for the MOC. If $\hat{T}(\psi)$ is the potential temperature averaged around each streamline, then the part of $\mathbf{H}$ given by $L_w(\mathbf{u}^*\hat{T})$ does not contribute to the northward heat transport. (Mathematically this can be seen by integrating the northward component of $L_w(\mathbf{u}^*\hat{T})$ vertically over the total depth and using the fact that $\psi = 0$ at the top and bottom of the ocean; physically this is because for this component of $\mathbf{H}$, the potential temperature of the water that is advected northward is the same as that which is returned southward, indicating no net heat transport). *Boccaletti et al.* [2005] therefore recommend replacing $\mathbf{H}$ by

$$\mathbf{H}_{\mathbf{bocc}} = \mathbf{H} - L_w\left(\mathbf{u}^*\hat{T}\right). \tag{3}$$

[5] Noting that $\nabla \cdot \mathbf{H}_{\mathbf{bocc}} = 0$, it is possible to define a stream function ϕ_{bocc} such that

$$\mathbf{H}_{\mathbf{bocc}} = \mathbf{H} - L_w\left(\mathbf{u}^*\hat{T}\right) = -\mathbf{i} \times \nabla\phi_{bocc}. \tag{4}$$

[6] *Boccaletti et al.* [2005] refer to ϕ_{bocc} as the heat function. They note that the value of ϕ_{bocc} at the surface is the same as the northward heat transport. Contours of ϕ_{bocc} therefore intersect the surface at latitudes where the northward heat transport is the same, and indicate the pathways

[1]Department of Oceanography, Dalhousie University, Halifax, Nova Scotia, Canada.

0094-8276/07/2007GL031427

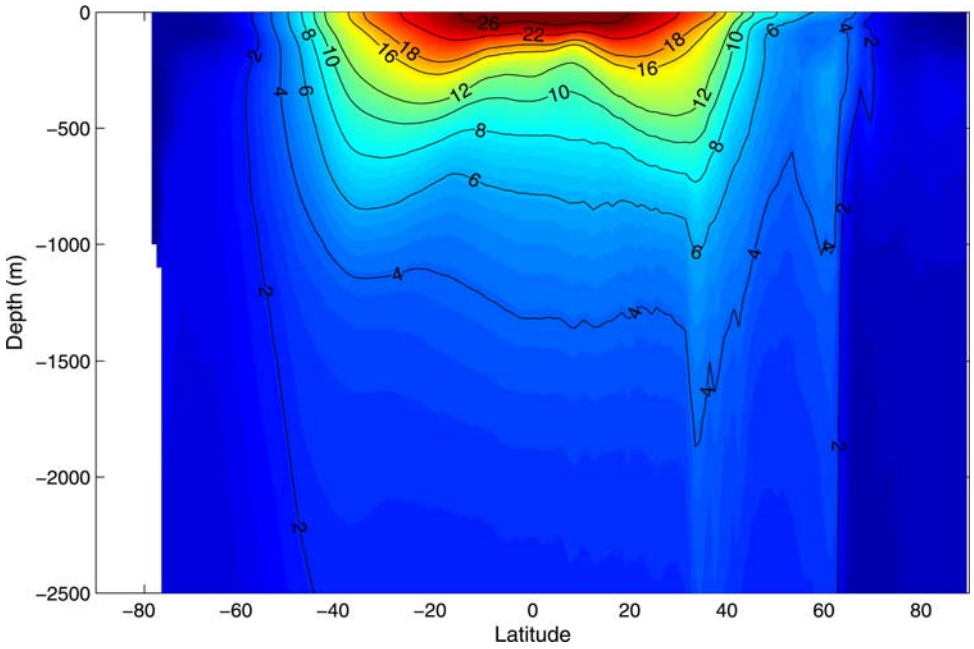

Figure 1. Zonally-averaged potential temperature (°C) from *Levitus et al.* [1998].

by which heat is redistributed in the ocean, from where heat enters (regions where the northward heat transport is increasing) to where heat exits (regions where the northward heat transport is decreasing).

2.2. The Generalized Heat Function

[7] We now present an alternative approach and define what we call "the generalized heat function". We begin by considering the heat budget for the volume of water bounded by the sea surface and a given isentrope $\bar{T} = T_o$, the isentropes being defined after zonal and time averaging at fixed height (see Figure 1). As noted by *Greatbatch et al.* [2007], the advection term in (1), given by $L_w(\mathbf{u}^*\bar{T})$, drops out of the balance and makes no contribution to the heat budget, a result that derives from *Walin* [1982]. Physically, this is because the heat content of the water that is advected into the control volume is the same as that which is advected out, leaving no net contribution. The resulting balance is given by

$$\int_s L_w[\mathbf{K}\nabla\bar{T}]\cdot\hat{\mathbf{n}}ds = \mathcal{H}, \tag{5}$$

where the integral is taken along the isentrope $\bar{T} = T_o$, $\hat{\mathbf{n}}$ is a unit vector perpendicular to the isentrope and pointing towards lower potential temperature, s is distance measured along the isentrope and $\mathcal{H}$ is the flux of heat through the sea surface between the latitudes either side of the equator where the $\bar{T} = T_o$ isentrope outcrops. (5) suggests defining what we shall call the generalized heat function by

$$\phi(s,\bar{T}) = \phi(0,\bar{T}) - \int_0^s L_w[\mathbf{K}\nabla\bar{T}]\cdot\hat{\mathbf{n}}ds, \tag{6}$$

where the integral is taken along the $\bar{T}$ contour and distance is measured from the surface in the southern hemisphere where $s = 0$. $\phi(0, \bar{T})$ is the northward heat transport at the latitude where the $\bar{T}$ isentrope intersects the surface in the southern hemisphere and the integral constraint (5) ensures that the value of ϕ where the $\bar{T}$ isentrope intersects the surface in the northern hemisphere (see Figure 1) is the northward heat transport at that latitude, therefore ensuring consistency. It is also possible to show that ϕ is a stream function for the heat transport vector

$$\mathbf{H} + \mathbf{i}\times\nabla[\psi\bar{T}] = -\mathbf{i}\times\nabla\phi, \tag{7}$$

showing the connection with the *Boccaletti et al.* [2005] approach (see equation (4)), but also showing that the generalized heat function, as defined by (6), is not identical to that defined by *Boccaletti et al.* [2005]. The generalized heat function is appealing because it shows the connection between the redistribution of heat in the ocean and ocean mixing. In particular, the generalized heat function, ϕ, is constant along isentropes if the mixing of heat across the isentrope, given by $[\mathbf{K}\nabla\hat{T}]\cdot\hat{\mathbf{n}}$ is zero. In fact, (6) makes it clear that changes in ϕ along an isentrope occur only in the presence of mixing. An advantage of the form given by (7) is that whereas (6) involves integration of ϕ along an isentrope, (7) avoids this complication and we suggest that (7) be used when diagnosing the generalized heat function from a model. Furthermore, the mixing present in models is often numerical in nature [e.g., *Griffies et al.*, 2000] and so is often not known exactly. (7) avoids this difficulty. Care is nevertheless required in the numerical formulation of the second term on the right hand side of (7) to ensure an accurate diagnosis of the heat function, and the precise formulation will depend on the particular model being used.

3. Results

[8] To illustrate the generalized heat function, we have integrated (6) along the isentropes shown in Figure 1 (i.e., the observed, zonally-averaged potential temperature field

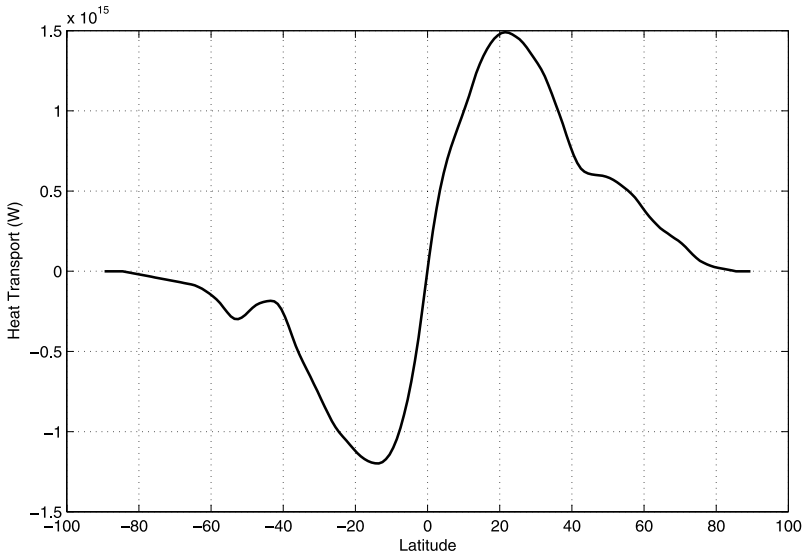

Figure 2. The northward net heat transport based on the work by *Grist and Josey* [2003].

averaged at fixed height) using a specified northward heat transport for the value of ϕ at the surface. For simplicity, we specify the mixing tensor **K** using a scalar dia-isentropic diffusivity, κ. Two different scenarios are considered. In the first (Scenario I) κ is chosen to be a function of $\bar{T}$, and so while taking a uniform value along any given isentrope, can vary from one isentrope to another. The functional dependence of κ on $\bar{T}$ is chosen to ensure consistency with the specified northward heat transport at the surface (i.e. to ensure that (5) is satisfied). Values of κ are typically between 0.5 and 2×10^{-4} m^2 s^{-1}. In the second scenario (Scenario II), the same procedure is adopted except that κ is given a value of 10^{-5} m^2 s^{-1} below 100 m depth, as commonly observed in the ocean thermocline [*Ledwell et al.*, 1993] but becomes a function of $\bar{T}$ in the upper 100 m where it takes much larger values, typically ranging from 0.5 to 2×10^4 m^2 s^{-1}. As in Scenario I, the value of κ in the top 100 m is chosen to ensure consistency with the specified northward heat transport so that (5) is satisfied. This choice for κ is a simple way to mimic the eddy-induced mixing near the surface that *Greatbatch et al.* [2007] have argued plays an important role in closing the ocean heat budget. Physically, the eddy-induced diffusivity near the surface results from the interaction between the eddies and the atmosphere within the surface mixed layer [see *Tandon and Garrett*, 1996; *Zhai and Greatbatch*, 2006a, 2006b].

[9] To carry out the diagnosis of ϕ, potential temperature is used as the vertical coordinate. A vertical resolution of 0.5°C is used over the potential temperature range 2°C to 28°C. For the northward heat transport we use the product of *Grist and Josey* [2003], modified to ensure that the northward heat transport is zero at both poles. This is accomplished by adding 5 W m^{-2} heat loss uniformly over the global ocean. The resulting global northward heat transport is shown in Figure 2 and is comparable within error bars to previous estimates from hydrographic data [e.g., *Ganachaud and Wunsch*, 2000]. Starting from its surface value in the southern hemisphere, that is the northward heat transport at the corresponding latitude, the generalized heat function ϕ is integrated northward along each isentrope by subtracting the dia-isentropic heat flux associated with κ, according to (6). When the integration of ϕ reaches the surface in the northern hemisphere, its value equals the northward heat transport at the latitude of the outcropping, a requirement ensured in both scenarios by the choice of κ. The generalized heat function ϕ in Scenario I is shown in Figure 3a after it is converted back to height coordinates. There are two shallow cells in the subtropics, which correspond to the heat carried by the wind-driven circulation. The opposite signs of the cells in opposite hemispheres reflects the fact that heat is gained by the ocean in the tropics and is then carried poleward where it is lost to the atmosphere, mostly in the western boundary current regions and associated with the big drop in the poleward heat transport between 20° and 40° each side of the equator in Figure 2. The other feature of Figure 3a is the yellow tongue extending southward across the equator at a depth between 500 m and 1000 m, below the wind-driven cells. This feature can also be seen Figure 1c of *Boccaletti et al.* [2005] and is the signature of the heat transport associated with the spreading of North Atlantic Deep Water (NADW). Overall, even in this diffusive scenario, the global heat transport has a shallow vertical structure and is dominated by the wind-driven cells. We now turn to Scenario II (Figure 3b), which we consider to be more appropriate for the real ocean. The heat transport associated with the spreading of NADW now appears as a pronounced reddish tongue between 500 m and 1000 m depth extending all the way to the southern hemisphere. Note that positive values of ϕ do not reach the surface in the southern hemisphere, and a large contribution from the eddy-induced mixing in the top 100 m is required to make ϕ negative at the surface, consistent with the net southward heat transport at these latitudes (Figure 2). The heat transport associated with the spreading of NADW, i.e., the reddish tongue, has a strength approaching 0.4 PW (1 PW = 10^{15} W) and is consistent with the model study of *Boccaletti et al.* [2005]. The negative values of ϕ below the red tongue likewise extend to the northern hemisphere, with a value of slightly larger than 0.1 PW, and correspond to the spreading of Antarctic

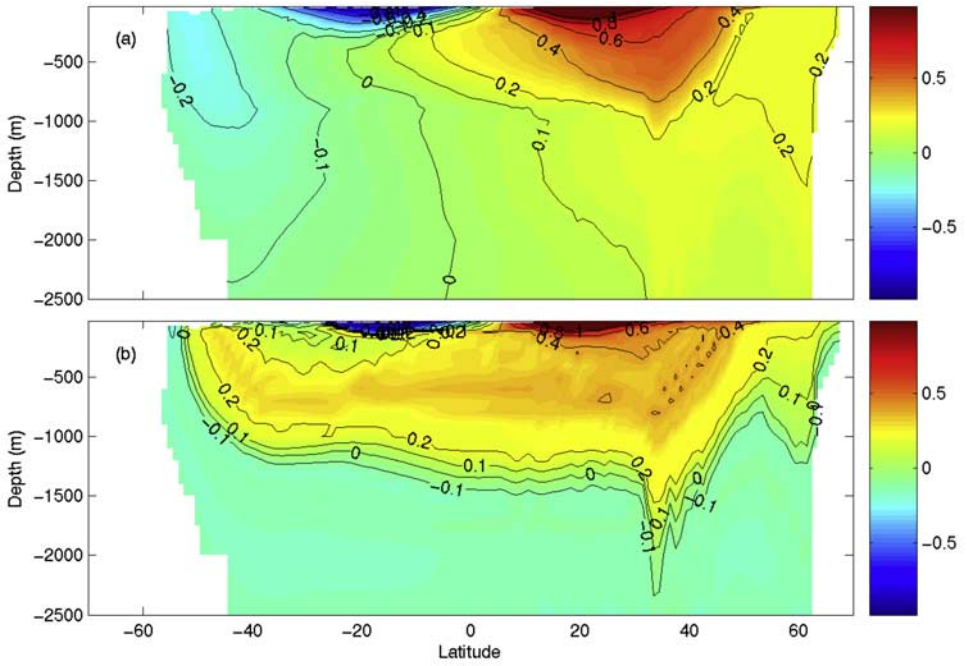

Figure 3. The generalized heat function (a) using a uniform value of κ on each isentrope and (b) using $K = 10^{-5}$ m^2 s^{-1} below 100 m depth. The units are PW. It should be noted that the heat function is plotted only on isentopes in the range 2°C to 28°C and above 2500 m depth.

Bottom Water. Since mixing is very weak in Scenario II below 100 m, the generalized heat function follows closely the isentropes (see, especially, the 4°C isentrope in Figure 1), i.e., $J(\phi, \hat{T}) \approx 0$. Meanwhile, we also note that the wind-driven cells are shallower in Scenario II, and mostly confined in the upper 100 m. This approaches the limit described by *Greatbatch et al.* [2007], where the surface heat input is balanced by eddy-induced mixing in the surface mixed layer. Several sensitivity studies have been carried out to test the origins of the transhemispheric heat flux associated with the spreading of NADW. The positive tongue exists, with a weaker strength, even in a case where the surface heat flux, potential temperature distribution and κ are set to be symmetric across the equator, demonstrating the role played by the variable zonal width of the ocean basins. For example, if eddy-induced mixing in both hemispheres is of the same efficiency, then the dia-isentropic heat flux associated with eddy-induced mixing will be much larger in the southern hemisphere, where the ocean covers a much larger percentage of each latitude band.

4. Summary and Discussion

[10] In this letter, we have extended the work of *Boccaletti et al.* [2005] and defined what we call the generalized heat function. Different from the more empirical approach taken by *Boccaletti et al.* [2005], the generalized heat function is both unique and physically appealing. The underpinning is the integral constraint derived by *Walin* [1982] in which the net surface heat input to the volume of water above by a mean isentrope is balanced by the mixing of heat across that isentrope. The generalized heat function, ϕ, is computed by integrating the dia-isentropic heat flux associated with mixing along each isentrope, with its surface value being the total northward heat transport at the latitude of the outcroppings. Therefore, changes in ϕ along an isentrope occur only in the presence of mixing. To illustrate the generalized heat function, we have carried out several experiments using the global data of *Levitus et al.* [1998], by specifying the northward heat transport using the work of *Grist and Josey* [2003], and adjusting the dia-isentropic mixing distribution to ensure that the integral constraint is satisfied. In Scenario I, where the dia-isentropic diffusivity is taken to be uniform along each isentrope, we find two intense shallow wind-driven cells in the subtropics associated with midlatitude subduction and equatorial upwelling [*Boccaletti et al.*, 2005]. The signature of the northward heat transport associated with the spreading of North Atlantic Deep Water can be seen beneath the wind-driven cells. However, since mixing is relatively large in the thermocline in this scenario, the generalized heat function is rather diffusive in the ocean interior. In the second scenario, mixing takes a value of 10^{-5} m^2 s^{-1} below 100 m depth as commonly observed in the main thermocline, and much larger values in the upper 100 m, mimicking eddy-induced mixing in the surface mixed layer. In this scenario, the generalized heat function follows closely the isentropes in the ocean interior because of the low level of mixing. The northward heat transport associated with the spreading of North Atlantic Deep Water (NADW) is much more pronounced, with a strength approaching 0.4 PW, consistent with the model of *Boccaletti et al.* [2005]. Meanwhile, the heat transport by the wind-driven cells is shallower and mostly confined to the top 100 m. We note that this scenario corresponds to the limit considered by *Greatbatch et al.* [2007] in which almost all the surface heat input is balanced by eddy-induced mixing associated with the interaction between the eddies and the atmosphere in the surface mixed

layer. Additional sensitivity studies show that the variable zonal width of the ocean basins plays an important role in the origin of the transhemispheric heat flux associated with the spreading of NADW.

[11] Finally, we note that the approach taken here to defining the heat function can, in principal, be extended to define a similar function for any tracer. In fact, the general concept of a "heat function" or "tracer function" is not new and has been used in the meteorology community for some time (for examples, see *Peixoto and Oort* [1992]). The generalized heat function, and other related tracer functions, are potentially powerful diagnostics for use with climate models and ocean observations.

[12] **Acknowledgments.** This work has been funded by R.J.G.'s NSERC Discovery Grant. R.J.G. is grateful to Klaus Fraedrich for pointing out the reference to *Peixoto and Oort* [1992]. The authors are also grateful to the Ocean University of China for their hospitality through the 111 project (B07036) during a recent visit when this paper was being written.

References

Alley, R. B., et al. (2003), Abrupt climate change, *Science*, *299*, 2005–2010.

Boccaletti, G., R. Ferrari, A. Adcroft, D. Ferreira, and J. Marshall (2005), The vertical structure of the ocean heat transport, *Geophys. Res. Lett.*, *32*, L10603, doi:10.1029/2005GL022474.

Bryan, K. (1962), Measurements of meridional heat transport by ocean currents, *J. Geophys. Res.*, *67*, 3403–3414.

Ganachaud, A., and C. Wunsch (2000), Improved estimates of global ocean circulation, heat transport and mixing from hydrological data, *Nature*, *408*, 453–457.

Gent, P., J. Willebrand, T. J. McDougall, and J. C. McWilliams (1995), Parameterizing eddy-induced tracer transports in ocean circulation models, *J. Phys. Oceanogr.*, *25*, 463–474.

Greatbatch, R. J., X. Zhai, C. Eden, and D. Olbers (2007), The possible role in the ocean heat budget of eddy-induced mixing due to air-sea interaction, *Geophys. Res. Lett.*, *34*, L07604, doi:10.1029/2007GL029533.

Griffies, S. M., R. C. Pacanowski, and R. W. Hallberg (2000), Spurious diapycnal mixing associated with advection in a z-coordinate ocean model, *Mon. Weather Rev.*, *128*, 538–564.

Grist, J. P., and S. A. Josey (2003), Inverse analysis adjustment of the SOC air-sea flux climatology using ocean heat transport constraints, *J. Clim.*, *16*, 3274–3295.

Hall, M. M., and H. L. Bryden (1982), Direct estimates and mechanisms of ocean heat transport, *Deep Sea Res.*, *29*, 339–359.

Ledwell, J. R., A. J. Watson, and C. S. Law (1993), Evidence for slow mixing across the pycnocline from an open ocean tracer release experiment, *Nature*, *364*, 701–703.

Levitus, S., et al. (1998), *World Ocean Database 1998*, vol. 1, U. S. Govt. Print. Off., Washington, D. C.

Peixoto, J. P., and A. H. Oort (1992), Physics of Climate, 520 pp., Am. Inst. of Phys., College Park, Md.

Roemmich, D., and C. Wunsch (1985), Two transatlantic sections: meridional circulation and heat flux in the subtropical North Atlantic Ocean, *Deep Sea Res.*, *32*, 619–664.

Tandon, A., and C. Garrett (1996), On a recent parameterization of mesoscale eddies, *J. Phys. Oceanogr.*, *26*, 406–411.

Walin, G. (1982), On the relation between sea-surface heat flow and thermal circulation in the ocean, *Tellus*, *34*, 187–195.

Wunsch, C. (2006), Abrupt climate change: An alternative view, *Quat. Res.*, *65*, 191–203.

Zhai, X., and R. J. Greatbatch (2006a), Inferring the eddy diffusivity for heat in the surface mixed layer using satellite data, *Geophys. Res. Lett.*, *33*, L24607, doi:10.1029/2006GL027875.

Zhai, Z., and R. J. Greatbatch (2006b), Surface eddy diffusivity for heat in a model of the northwest Atlantic Ocean, *Geophys. Res. Lett.*, *33*, L24611, doi:10.1029/2006GL028712.

R. J. Greatbatch and X. Zhai, Department of Oceanography, Dalhousie University, Halifax, NS, Canada B3H 4J1. (xiaoming.zhai@phys.ocean.dal.ca)